

1 **Robust identification of deletions in exome and genome sequence data based on**
2 **clustering of Mendelian errors**

3

4 **Authors:** Kathryn B. Manheimer¹, Nihir Patel¹, Felix Richter¹, Joshua Gorham⁴, Angela
5 C. Tai⁴, Jason Homsy^{4,12}, Marko T. Boskovski¹³, Michael Parfenov⁴, Elizabeth
6 Goldmontz^{5,6}, Wendy K. Chung^{7,8}, Martina Brueckner^{15,16}, Martin Tristani-Firouzi⁹,
7 Deepak Srivastava^{10,11}, Jonathan G. Seidman⁴, Christine E. Seidman^{4,14}, Bruce D.
8 Gelb^{1,2,3}, Andrew J. Sharp^{1,2*}

9

10

11 **Affiliations:**

12

13 ¹Mindich Child Health and Development Institute and Departments of ²Genetics and
14 Genomic Sciences and ³Pediatrics, Icahn School of Medicine at Mount Sinai, New York,
15 NY, USA, ⁴Department of Genetics, Harvard Medical School, Boston MA, USA,
16 ⁵Department of Pediatrics, The Perelman School of Medicine, University of
17 Pennsylvania, Philadelphia, PA, USA, ⁶Division of Cardiology, The Children's Hospital
18 of Philadelphia, The University of Pennsylvania Perelman School of Medicine,
19 Philadelphia, PA, USA, Departments of ⁷Pediatrics and ⁸Medicine, Columbia University
20 Medical Center, New York, NY, USA, ⁹Department of Pediatric Cardiology, University of
21 Utah, Salt Lake City, UT, USA, ¹⁰Department of Pediatrics, UCSF, San Francisco, CA,
22 USA, ¹¹Gladstone Institutes, San Francisco, CA, USA, ¹²Cardiovascular Research
23 Center, Massachusetts General Hospital, Boston, MA, USA, ¹³Division of Cardiac

24 Surgery, The Brigham and Women's Hospital, Harvard Medical School, Boston, MA,
25 USA, ¹⁴Department of Medicine (Cardiology), Brigham and Women's Hospital, Boston,
26 MA and the Howard Hughes Medical Institute, Chevy Chase, MD, USA, ¹⁵Genetics and
27 ¹⁶Pediatrics, Yale University School of Medicine, New Haven, CT, USA

28

29 *Address for correspondence: Andrew J. Sharp, Department of Genetics and Genomic
30 Sciences, Mount Sinai School of Medicine, Hess Center for Science and Medicine,
31 1470 Madison Avenue, Room 8-116, Box 1498, New York, NY 10029 USA. Telephone:
32 +1-212-824-8942, Fax: +1-646-537-8527, Email: andrew.sharp@mssm.edu

33

34

35 **Abstract**

36 Multiple tools have been developed to identify copy number variants (CNVs) from whole
37 exome (WES) and whole genome sequencing (WGS) data. Current tools such as
38 XHMM for WES and CNVnator for WGS identify CNVs based on changes in read depth.
39 For WGS, other methods to identify CNVs include utilizing discordant read pairs and
40 split reads and genome-wide local assembly with tools such as Lumpy and SvABA,
41 respectively. Here, we introduce a new method to identify deletion CNVs from WES and
42 WGS trio data based on the clustering of Mendelian errors (MEs). Using our Mendelian
43 Error Method (MEM), we identified 127 deletions (inherited and *de novo*) in 2,601 WES
44 trios from the Pediatric Cardiac Genomics Consortium, with a validation rate of 88% by
45 digital droplet PCR. MEM identified additional *de novo* deletions compared to XHMM,
46 and also identified sample switches, DNA contamination, a significant enrichment of
47 15q11.2 deletions compared to controls and eight cases of uniparental disomy. We
48 applied MEM to WGS data from the Genome In A Bottle Ashkenazi trio and identified
49 deletions with 97% specificity. MEM provides a robust, computationally inexpensive
50 method for identifying deletions, and an orthogonal approach for verifying deletions
51 called by other tools.

52

53 **Keywords:** copy number variant identification, whole exome sequencing, whole
54 genome sequencing, UPD

55

56

57

58

59 **Introduction**

60

61 Structural variation (SV), particularly *de novo* deletions, has been implicated in many
62 human diseases including autism spectrum disorders, developmental delay,
63 schizophrenia and congenital heart disease (Weischenfeldt et al., 2013; Gilissen et al.,
64 2014; Glessner et al., 2014; Szatkiewicz et al., 2014; Bandler et al., 2015). Previously
65 identified using microarrays, many tools have been developed in the past ten years to
66 identify SV from next generation sequencing (NGS) data (Tattini et al., 2015). These
67 tools utilize three main lines of evidence to detect SV: changes in read depth,
68 discordant read pairs and split reads. Assembly methods including genome-wide local
69 assembly and *de novo* assembly are also available (Weisenfeld et al., 2014; Wala et al.,
70 2017).

71

72 With respect to whole exome sequencing (WES) data, one tool to identify copy number
73 variants (CNVs) is XHMM, which identifies changes in normalized read depth within a
74 cohort (Fromer and Purcell, 2014). Although widely used for identifying CNVs from WES
75 data, XHMM has several limitations, including a minimum cohort size and the
76 requirement that CNVs must include at least three exons. Typically, ~20% of putative
77 CNVs identified by XHMM fail to be confirmed, and its sensitivity is limited (Glessner et
78 al., 2014). For example, one study that used both XHMM and SNP arrays to identify *de*
79 *novo* CNVs found that XHMM failed to detect 63% of CNVs identified by the SNP array

80 (Glessner et al., 2014). The limited sensitivity of XHMM stems from the limitations of
81 WES, some of which can be overcome with whole genome sequencing (WGS).

82

83 Multiple tools have been developed to identify SV from WGS data including CNVnator
84 and Lumpy (Abyzov et al., 2011; Layer et al., 2014). While CNVnator identifies CNVs
85 based on changes in normalized read depth (Abyzov et al., 2011), Lumpy utilizes
86 discordant read pairs and split reads to identify deletions, duplications and other types
87 of SVs (Layer et al., 2014). Lumpy is often used in combination with CNVnator to take
88 into account changes in read depth. In order to estimate the sensitivity and false
89 discovery rate (FDR), SVs identified by CNVnator and Lumpy were both compared to
90 SVs identified in the 1000 Genomes Project by other SV callers (e.g., Delly, Pindel).
91 Although both tools are reported to have a low FDR (0.4 – 3%) and high sensitivity (60 –
92 90%) (Abyzov et al., 2011; Layer et al., 2014), the accuracy of these tools diminishes
93 when used for identifying *de novo* SV (Kloosterman et al., 2015). This problem results
94 from a lack of sensitivity when identifying SVs: false negatives in parental samples lead
95 to a high false positive rate for calling *de novo* SV, creating a significant challenge when
96 attempting to identify *de novo* events that are potentially pathogenic.

97

98 Here, we describe a novel approach called the Mendelian Error Method (MEM) to
99 identify and/or validate deletion SV in trios with WES and WGS data. MEM is based on
100 the principle described in McCarroll et al. 2006 (McCarroll et al., 2006), where the
101 presence of a heterozygous deletion reduces the underlying genotype to a hemizygous
102 state. As genotype callers such as GATK assign diploid genotypes to autosomal loci,

103 regions of heterozygous deletion are erroneously assigned homozygous genotypes. In
104 the context of a trio design, variants within heterozygous deletions frequently display
105 Mendelian errors as a result of this genotype mis-assignment (illustrated in Figure 1).
106 We, therefore, hypothesized that clusters of Mendelian errors could be used as a robust
107 signal for the presence of underlying deletions in sequencing data from trios. We
108 applied MEM to both WES and WGS trio data from the Pediatric Cardiac Genomic
109 Consortium (PCGC) and compared results to deletions identified by XHMM, CNVnator
110 and Lumpy. Overall, our results show that MEM identifies both inherited and *de novo*
111 deletions with a positive predictive value (PPV) exceeding 90%, and identifies additional
112 *de novo* deletions that are missed by other SV callers.

113

114 **Methods**

115

116 *WES and WGS in cases with CHD*

117 Probands were recruited from 10 centers in the United States and United Kingdom as
118 part of the Congenital Heart Disease Genetic Network study of the PCGC as described
119 previously (Homsy et al., 2015). Cases (n=2,601) were subject to WES at the Yale
120 Center for Genome Analysis as described previously (Homsy et al., 2015), with a mean
121 depth of 107x. All genomic coordinates quoted are based on human genome
122 hg19/build 37. Variants were called following the n+1 protocol from GATK.

123

124 Three hundred and fifty probands and their parents from the PCGC were selected for
125 WGS; of note 332 also have WES data. Cases were sequenced at the Broad Institute

126 (n=25), New York Genome Center (n=25) and Baylor College of Medicine Human
127 Genome Sequencing Center (n=300). Samples were sequenced with PCR-free library
128 preparation (n=325) or with SK2-IES (n=25) to a mean depth of 30x on Illumina HiSeq X
129 Ten sequencers. Variants were called by GATK HaplotypeCaller (version 3.3.2)
130 following GATK best practices for n+1 joint calling
131 (<https://software.broadinstitute.org/gatk/best-practices/>).

132
133 *WES and WGS of healthy population cohort*
134 Trios representing a typical population cohort (n=1,683) were provided by the Simons
135 Foundation Autism Research Initiative Simplex Collection. Simplex families (two
136 unaffected parents, one child with autism spectrum disorder, and one unaffected sibling)
137 underwent WES using DNA extracted from peripheral blood cells, with a mean depth of
138 117x (O'Roak et al., 2011; Sanders et al., 2012; Iossifov et al., 2014). Trios of
139 unaffected siblings and parents served as a typical population cohort for comparison.

140
141 Five hundred and nineteen quartet families selected from the Simons Simplex
142 Collection (SSC) underwent WGS at the New York Genome Center. Samples were
143 sequenced with either a PCR-based library preparation on an Illumina Hi-Seq 2000
144 (n=39) or PCR-free library preparation on an Illumina HiSeq X Ten (n=480). Sequencing
145 was performed with 150-bp paired reads with median coverage of 37.8x per individual.
146 Detailed information regarding this cohort can be found in Werling *et al.* (Werling et al.,
147 2017)

148

149 Variants were called using GATK HaplotypeCaller (version 3.1-1-g07a4bf8, n=19,
150 version 3.2-2-gec30ce, n=21, version 3.4-0-g7e26428, n=479). GATK best practices
151 (<https://software.broadinstitute.org/gatk/best-practices/>) were followed. Trios comprising an
152 unaffected sibling and their parents were used as a typical population cohort for
153 comparison in this study with permission from the SSC.

154

155 *Genome in a Bottle (GIAB) WGS with Illumina*

156 The GIAB Ashkenazi Jewish (AJ) trio was subject to WGS using both short and long
157 read methodologies. 148-bp paired-end reads were generated with an Illumina Hiseq
158 instrument. Reads were aligned with BWA-mem (details in Zook *et al.*, 2016) (Zook et
159 al., 2016). Variants were called by GATK HaplotypeCaller (version 3.3.2) following
160 GATK best practices using n+1 joint calling.

161

162 *GIAB deletions for AJ trio*

163 GIAB provided draft benchmark structural variants (SVs) for the AJ trio (v0.3.0a). SVs
164 from 119 different tools were compared and merged using the tool SURVIVOR (Jeffares
165 et al., 2017), which required the breakpoints to be within 1000 bp. Deletions identified
166 by a minimum of two tools were compared to deletions identified by MEM using
167 bedtools and required a 20% reciprocal overlap.

168

169 *Mendelian Error Method (MEM) Pipeline – Figure 2*

170

171 *1. Extract Mendelian errors (MEs) from WES and WGS VCFs*

172 MEs were extracted based on genotypes reported in the joint VCF produced by GATK
173 best practices, using in-house perl scripts or vcftools. Table S1 includes the eight
174 scenarios considered as MEs that could represent a deletion.

175

176 *2. Filtering*

177 Variants in PCGC, GIAB and SSC trios were filtered using the following criteria: read
178 depth ≥ 10 , genotype quality >60 for WES and >30 for WGS (Table S2). B allele
179 frequency (BAF, defined as the alternate allele depth/total depth) was calculated for
180 heterozygous SNVs, and those with a BAF <0.25 or >0.75 were excluded. Regions
181 overlapping segmental duplications obtained from the UCSC Genome Browser track
182 were excluded. CNVs with a minor allele frequency ≥ 0.05 in European, African or East
183 Asian ancestry as identified in Conrad *et al.* were excluded (Conrad *et al.*, 2012). For
184 WGS, SNVs with a mappability score <1 were excluded, based on the UCSC Genome
185 Browser track “Alignability of 100mers by GEM from ENCODE/CRG(Guigo)”. Regions
186 with tandem repeats, taken from the UCSC Genome Browser track “Simple Repeats”
187 and expanded ± 5 bp, were excluded. The Hardy Weinberg equilibrium (HWE) statistic
188 was calculated using vcftools for SNVs with a minimum allele frequency of 0.01 in
189 parents. Any SNVs with a HWE p-value equal to zero were removed.

190

191 *3. Sliding window analysis*

192 We generated 2-Mb windows with 95% overlap for WES analysis and 100-kb windows
193 with 90% overlap for WGS analysis using Bedtools (version 2.26.0) makewindows. In
194 house bash scripts utilizing Bedtools intersect were used to calculate the number of

195 MEs for each window. This was applied to each sample in the PCGC and SSC cohorts
196 separately.

197

198 For each unique window, the number of probands with MEs, the minimum number of
199 MEs, the maximum number of MEs and the average number of MEs per proband were
200 calculated for PCGC and SSC probands. We filtered for windows where the average
201 number of MEs per proband was >2 MEs.

202

203 *4. Comparison to population cohort*

204 Windows with MEs in PCGC cases were compared to corresponding windows in the
205 SSC population cohort. Windows with a ME cluster in three or more SSC probands
206 were excluded, except if the maximum number of MEs in cases was >5.

207

208 *5. Merge windows*

209 For each sample overlapping windows with MEs were merged to identify putative
210 deletion regions. The minimum, maximum and average number of MEs per window was
211 calculated for each region. The number of MEs in each putative deletion region was
212 calculated in SSC probands and regions with ME clusters as described in Step 4 were
213 removed from further analysis.

214

215 *6. Filter for ME clusters*

216 Finally, we filtered for regions with an average number of MEs per window >2 in cases.
217 We identified the first and last ME within each region and used these as the coordinates
218 for the putative deletions.

219

220 *Visualization*

221 1. XHMM

222 For putative deletions identified with MEM from the PCGC WES cohort, we extracted z-
223 scores of the PCA-normalized read depth for each exon from XHMM (Fromer and
224 Purcell, 2014). Putative deletions were inspected visually (Figure S1) and exons with z-
225 scores <-2 were considered candidates for deletions.

226

227 2. IGV

228 Integrated Genomics Viewer (IGV, version 2.3.34) pileup visualization was used as one
229 method for deletion validation. Variants were visualized in the proband and parents.
230 Deletions were excluded if any of the following aspects were detected: multiple reads
231 with quality scores of zero in child or parents, no clear drop of coverage in the proband,
232 or the presence of heterozygous SNVs in the proband.

233

234 *CNVnator*

235 CNVnator identifies CNVs in WGS data based on changes in normalized read depth
236 (Abyzov et al., 2011). Deletions were called for each case proband and the GIAB
237 proband with CNVnator (version 0.3.2) and genotyped for putative copy number within
238 the CNV regions on a scale from 0 – 3. We considered scores between 0.7 – 1.4 as

239 indicating a heterozygous deletion. *De novo* deletions were identified by filtering for a
240 score <1.4 in the child and >1.4 in the parents. We overlapped putative deletions in
241 WGS cases identified using MEM with *de novo* deletions identified by CNVnator using
242 Bedtools intersect, requiring a 25% reciprocal overlap. In the AJ trio, we overlapped
243 putative deletions identified with MEM with both inherited (proband genotype <1.4) and
244 *de novo* deletions called by CNVnator, and considered all intersections with at least 1
245 bp of overlap.

246

247 *Lumpy*

248 Lumpy identifies SVs based on discordant read pairs and split-reads (Layer et al.,
249 2014). Deletions were called for each case proband and the GIAB proband with Lumpy
250 (version 0.2.13) and genotyped using SVtyper (version 0.0.4). *De novo* deletions were
251 identified based on proband and parent genotypes. We overlapped PCGC WGS MEM
252 deletions with Lumpy *de novo* deletions in the same manner as CNVnator. In the AJ
253 trio, we overlapped putative deletions identified with MEM with both inherited and *de*
254 *novo* deletions by Lumpy, and considered all intersections with at least 1 bp of overlap.

255

256 *SvABA*

257 Deletions were called with SvABA from 350 WGS trios based on genome-wide local
258 assembly (Wala et al., 2017). Default parameters were employed to identify putative
259 copy number variants, which were further validated by IGV visualization prior to digital
260 droplet PCR analyses.

261

262 *Deletion validation*

263 Digital droplet PCR (ddPCR) was used to validate MEM WES deletions and WGS *de*
264 *novo* deletions identified by CNVnator and Lumpy, as previously reported (Mazaika and
265 Homsy, 2014) with the following modification. PCR primers that amplified a portion of
266 the putative CNV were designed to avoid homopolymer runs or probes that begin with
267 G. PCR-positive droplets were identified by EvaGreen dye (DNA-bound emission at
268 500/533 nm). CNV product positive droplets were EvaGreen dye positive, VIC
269 negative. A VIC probe targeting the RPP30 gene was used as reference. Reaction
270 mixtures of 20 μ L volume comprising ddPCR Master Mix (Bio-Rad), relevant forward and
271 reverse primers and probe(s) and 50ng of DNA were prepared, ensuring that<40% of
272 the 5000-10000 droplets ultimately produced were positive for Evagreen dye and/or VIC
273 signal. For *de novo* CNV confirmations, DNA from the subject with CHD and parents
274 was used. After thermal cycling, plates were transferred to a droplet reader (Bio-Rad)
275 that flows droplets single-file past a 2-color fluorescence detector. Differentiation
276 between droplets that contain target and those that did not was achieved by applying a
277 global fluorescence amplitude threshold in QuantaSoft (Bio-Rad). The threshold was set
278 manually based on visual inspection at approximately the mid-point between the
279 average fluorescence amplitude of positives and negative droplet clusters on each of
280 the EvaGreen dye and VIC channels. Confirmed CNV duplications had \approx 50% increase
281 in the ratio of positive to negative droplets, as did the reference channel. Conversely,
282 confirmed CNV deletions had approximately half the ratio of positive to negative
283 droplets, as did the reference channel. CNVs that were called, but were unable to be

284 confirmed or rejected due to ddPCR technical failure or DNA unavailability were
285 excluded from analysis.

286

287 **Results**

288

289 *MEM identifies inherited and de novo deletions from WES trios*

290 The MEM pipeline was used to analyze WES data from 2,601 PCGC trios and 1,683
291 healthy trios from the SSC. Windows with ME clusters in SSC probands were removed
292 as described in Methods in order to limit our findings to those of likely relevance to the
293 pathogenesis of congenital heart disease (CHD). MEM identified a final set of 171
294 merged and filtered regions containing putative deletions in the PCGC probands (Table
295 S3). We used the location of the first and the last ME in each region with a ME cluster to
296 define the minimal coordinates for the deletion. We utilized XHMM read depth data to
297 perform an initial assessment of the accuracy of our MEM deletion calls. The proband's
298 normalized XHMM z-scores for each exon within the deletion identified by MEM were
299 compared to the rest of the cohort (Figure S1). The presence of outlier negative z-
300 scores in the proband suggested a deletion. The parents' z-scores were also compared
301 to the rest of the cohort to determine if the deletion was inherited or *de novo*. In this
302 manner, 58 deletions were determined to be *de novo*, and 79 were noted to be
303 inherited. Of note, the exons in 13 ME clusters did not have negative normalized z-
304 scores, and seven ME clusters showed inconsistent scores, with some exons showing
305 reduced XHMM z-scores, while other exons were within the normal range (z-score >-2),
306 suggesting that these 20 calls could be false positives.

307

308 We directly compared the performance of MEM for the detection of *de novo* deletions
309 with that of XHMM. Fifty deletions were called by both tools, 46 by XHMM alone, and 25
310 by MEM alone (Figure 3A). Of note, the 25 MEM-exclusive deletions included 13 that
311 showed no reduction in z-scores with XHMM for proband or parents and, thus, could
312 represent either *de novo* deletions or false positives. We considered the size of the
313 deletions that MEM did and did not identify. For deletions ≥ 200 kb, MEM identified
314 100% of deletions, however for deletions < 200 kb MEM identified 24% of deletions
315 (Figure 3B). The 46 XHMM-exclusive deletions had a mean size of 35 kb and, therefore
316 due to an insufficient number of SNPs within them, could not be identified by MEM with
317 high recall.

318

319 From the 171 MEM deletions, 36 overlapped with deletions previously confirmed by
320 digital droplet PCR (ddPCR). For the remaining 135 deletions, we performed ddPCR,
321 which was successful for 109 deletions. Ninety-six out of 109 were confirmed as true
322 deletions, achieving a positive predictive value (PPV) of 88.1%. Surprisingly, the results
323 from ddPCR indicated that five of the regions with the ME cluster were inherited
324 duplications. Thus, overall 137/145 (94.5%) of ME clusters identified by MEM were
325 confirmed as true CNVs. Deletions identified as inherited by inspection of XHMM z-
326 score plots confirmed with a PPV of 86% (49/57 inherited, 3/57 *de novo*). From the
327 possible false positives, two out of eight deletion regions without negative normalized z-
328 scores in XHMM were confirmed, and four of six regions with inconsistent loss of exons

329 confirmed. Finally, 26 *de novo* deletions were confirmed, four exclusively identified by
330 MEM.

331

332 *Enrichment of deletions on chromosome 15q11.2*

333 With MEM, we identified 15 deletions (13 inherited, 2 *de novo*) ranging from 11 kb to 1
334 MB in the chromosome region 15q11.2 in PCGC probands. These deletions fall in a
335 known microdeletion region between breakpoints (BP) 1 and 2, with a population
336 frequency of 0.25% (Cafferkey et al., 2014). Deletions in this region occurred at a
337 frequency of 0.58% (15/2,601) in the PCGC cohort, and are therefore enriched
338 compared to the reported population frequency (binomial, $p=0.004$) and to SSC
339 probands, which had a deletion frequency of 0.24% (4/1,683) deletions in this region
340 (binomial, $p=0.002$).

341

342 *Identification of uniparental disomy (UPD) in WES trios by MEM*

343 Following ME extraction and applying quality filters (Table S1), the majority of trios had
344 between 0.6 – 2% of loci that were scored as MEs (Figure 4A). We identified eight
345 probands with an elevated rate of MEs distributed across an entire chromosome,
346 suggestive of possible uniparental disomy (UPD). Prior microarray experiments noted
347 UPD of chromosome 15 for one proband, and an extended region of homozygosity on
348 chromosome 16 for a second proband. However, there was no prior indication of UPD
349 in the other six cases.

350

351 All eight instances of UPD were classified as maternal heterodisomy, based on the
352 presence of heterozygous maternal SNPs. The heterodisomic inheritance was for
353 chromosomes 4 (x2), 8, 9, 14, 15 and 16 (x2). UPD was not found in any SSC
354 probands, and was therefore enriched in cases (binomial, $p=0.026$).

355

356 *MEs identify irregularities in WES trios*

357 We identified two other distinct ME patterns that were informative. Twenty trios had a
358 dramatically higher rate of MEs (~50% of all SNVs), which were distributed across every
359 chromosome (Figure 4D). Nearly all of the MEs were attributable to lack of inheritance
360 from one parent, suggesting either a sample switch or incorrect paternity.

361

362 Similarly, we observed an elevated, but lower, rate (20-30%) of MEs distributed across
363 the entire genome in six other probands (Figure 4C). We hypothesized that this pattern
364 might be due to DNA contamination, which was confirmed with the program
365 VerifyBamID (Jun et al., 2012).

366

367 All samples with likely sample mix-ups, DNA contamination or UPD were excluded from
368 further analysis.

369

370 *ME clusters are non-random in the genome*

371 Before applying MEM to WGS data, we first needed to determine if the increased SNV
372 density in WGS data relative to WES data could lead to ME clusters by chance alone.
373 To test this, we generated a null model of SNV clusters across the genome. We only

374 considered heterozygous SNVs, and also applied additional filters for genotypes
375 generated from WGS as shown in Table 1. After applying these quality filters, the
376 median number of MEs per proband among the 350 PCGC WGS trios was 317. We
377 then ran 1000 permutations of selecting 317 informative SNV positions from one trio,
378 assuming those were MEs, and implemented MEM with a 100-kb window and 10-kb
379 slide. We calculated the number of windows with SNV clusters divided by the number of
380 windows with at least 1 SNV. The null model had a mean of 0.3% of windows with a
381 SNV cluster (Figure S2). In contrast, 21.4% of windows with at least 1 ME among the
382 PCGC WGS probands had a ME cluster and they were infrequent across the genome
383 (Figure S2). From these results, we inferred that ME clusters in WGS were likely non-
384 random and were likely identifying underlying deletions.

385

386 *Mendelian error clusters identify deletions from GIAB Ashkenazi trio*
387 To test the robustness of MEM for calling deletions from WGS, we identified putative
388 deletions using MEM based on genotypes generated using Illumina short read WGS
389 data for an Ashkenazi Jewish (AJ) trio sequenced by the GIAB consortium (Zook et al.,
390 2016). We processed filtered SNV genotypes from the Illumina WGS data in this trio
391 using the parameters listed in Table 1 and searched for ME clusters. Using the MEM
392 pipeline we identified 32 putative deletions (Table S3) that contained an average of 9.4
393 MEs, with a mean size of 31.5 kb.

394

395 To determine the accuracy of the MEM deletion calls, we intersected them with draft
396 benchmark deletions provided by GIAB. Requiring a 20% reciprocal overlap between

397 deletions, 27/32 MEM deletions overlapped with those from GIAB. After removing the
398 20% overlap requirement 31/32 MEM deletions overlapped. The five deletions that did
399 not overlap by 20% were visualized in IGV, where we found evidence for a deletion in
400 4/5. Therefore, MEM identified deletions with 97% precision from WGS for the GIAB AJ
401 proband. Of note, one 215-kb MEM deletion overlapped two GIAB deletions.

402 Visualization in IGV confirmed the presence of two separate deletion events at this
403 locus, which the distribution of MEs also supports (Figure S3).

404

405 Next, we looked at the deletions identified by GIAB that MEM did not identify
406 (n=24,090). These do not include deletions in segmental duplication regions but do
407 include 14,690 deletions at tandem repeat loci. Due to the challenges of sequencing
408 tandem repeats with short read sequencing we would not expect MEM to accurately
409 identify deletions with tandem repeats, as variant calling is unreliable in these regions.

410 The MEM false negatives (FNs) had a median size of 39 bp and a mean size of 306 bp
411 and were attributable to inadequate number of MEs in those deletions as 93.5% did not
412 include any MEs before filtering. Only 1% of the MEM FNs were related, at least in part,
413 to the filtering of MEs, having >2 MEs prior to filtering.

414

415 We also compared the MEM calls for the AJ trio to calls from CNVnator and Lumpy. Of
416 the 32 MEM deletion calls, 27 (84%) and 23 (72%) overlapped with calls from CNVnator
417 and Lumpy, respectively. There were many calls from CNVnator and Lumpy that were
418 not made by MEM, however most of them contained no MEs. ME filtering accounted for
419 21% of FNs from CNVnator calls and 6% of FNs from Lumpy calls.

420

421 *MEM identifies deletions from WGS trios*

422 Based on the promising results from GIAB, we proceeded to apply the MEM pipeline to
423 identify deletions from 350 WGS case trios from the PCGC, and 517 healthy trios from
424 the SSC. From the PCGC trios, MEM identified 6,645 regions with ME clusters
425 (mean=19.1/proband) that ranged in size from 3 bp to 9 Mb, with a median size of 2.9
426 kb and a mean size of 20 kb (Table S3). Eleven percent of regions included exons. We
427 used the first and last MEs as coordinates for the putative deletions. For 332 PCGC
428 trios that have both WES and WGS data we compared the deletions identified by MEM
429 from both data sets. MEM identified 11 deletions from WES, all of which were detected
430 by MEM with WGS. All of the deletions were the same size or larger when detected by
431 WGS except for one. This is expected as the increased SNP density of WGS provides
432 more informative sites for MEM, thus facilitating a better estimate of the deletion size.

433

434 To determine if the ME clusters in WGS data identified true deletions, we integrated
435 normalized read depth data from CNVnator. Each region was labeled with a CNVnator
436 score where 0 corresponds to a homozygous deletion, 0.7-1.5 to a heterozygous
437 deletion, 1.5-2.4 to being normally diploid and >2.4 to a duplication. The vast majority
438 (97%) of MEM deletions had a CNVnator score between 0.7 – 1.5 suggesting MEM was
439 identifying true heterozygous deletions (Figure S4). We visualized MEM deletion calls
440 with a CNVnator score >1.5 in IGV. Based on this manual curation, we concluded that
441 the majority (66%) were false positives, but 34% were heterozygous deletions: 10%
442 covering the entire region and 24% being either a deletion of a portion of the region or

443 two smaller deletions located close together. In addition, we visualized in IGV a test set
444 of MEM deletions with a range of CNVnator scores. The vast majority of false positives
445 (93.5%) had a score of 1.5 or greater, while 100% of the true or possible deletions had
446 a score between 0.7 and 1.5 (Figure S5). Overall, our comparison with read depth data
447 supports a PPV of 92% (Supplementary Formula 1) for identifying heterozygous
448 deletions from WGS with MEM.

449

450 Next, we identified which MEM deletions were *de novo* based on the proband and
451 parents' CNVnator scores. We used two sets of filters (Table S4) and identified 37
452 putative *de novo* deletion calls (mean = 0.12 *de novo* deletions/proband) After
453 visualization in IGV, we determined that 20/37 represented likely true *de novo* deletions,
454 while 17 were inherited. We compared these to *de novo* deletions identified by
455 CNVnator, Lumpy and a third WGS tool called SvABA that uses genome-wide local
456 assembly to identify SV (Wala et al., 2017). The deletions called by the other SV tools
457 were confirmed by ddPCR. Of the 20 *de novo* deletions found by MEM, five were also
458 identified by CNVnator, Lumpy, and SvABA, three were identified by CNVnator and
459 SvABA but not Lumpy, and 12 were not found by the three other tools. Thirteen
460 additional *de novo* deletions were identified with a combination of CNVnator, Lumpy and
461 SvABA: all three tools but not MEM (n=7), CNVnator and SvABA (n=2), CNVnator and
462 Lumpy (n=1), CNVnator only (n=2), and SvABA only (n=1). None of these deletions,
463 which had a median size of 6.5 kb, included any MEs, suggesting MEM is less sensitive
464 for deletions smaller than ~10 kb in WGS.

465

466 *MEM is computationally efficient*

467 We compared the computational resources required for MEM and the other CNV
468 detection tools used in this study for deletion identification in one trio (Table 1). Runtime
469 and memory for all tools were based on the use of an Intel Haswell 2.4 GHz processor
470 with 64 GB memory and Cray nodes. We did not utilize parallelization for any of the
471 tools. Runtime and memory for MEM was calculated for Step 1 of the MEM pipeline (ME
472 extraction). All other steps in the MEM pipeline can be performed on the command line
473 and do not require significant time or memory. Of note, resources required for the
474 preliminary steps for all tools (DepthOfCoverage for XHMM, Samblaster for Lumpy, and
475 variant calling for MEM) were not included.

476

477 For WES, MEM required 5.5 sec and an average of 12 MB of memory per trio. XHMM
478 required 453 sec and on average 81 MB of memory. For WGS, MEM required 407 sec
479 and an average of 7 MB of memory per trio. CNVnator required 77,629 sec and, on
480 average, 709 MB of memory. Lumpy/SVTyper required 4,238 sec and an average of
481 4,898 MB of memory. SVTyper produced genotypes for deletions only and not other
482 types of SV (duplications, translocations, inversions). For both WES and WGS, MEM
483 performed significantly faster and required significantly less memory compared to other
484 CNV detection tools. Of note, ME extraction execution time grows sub-linearly based on
485 the number of trios present in the VCF, however average memory required does not
486 increase significantly.

487

488 **Discussion**

489 A variety of tools have been developed to identify CNVs including XHMM and CoNIFER
490 for WES, and CNVnator, Lumpy and SvABA for WGS. Each of these tools has
491 limitations such as a requirement for 50 samples, the need for extensive computational
492 resources, or that up to 20% of CNVs will fail to confirm. In addition, false negative calls
493 in parents lead to a high false positive rate for *de novo* deletion CNV calls, making the
494 identification of true *de novo* CNVs difficult and time intensive. As documented in this
495 report, we developed a novel method, MEM: the Mendelian Error Method, to identify
496 deletion CNVs based on ME clustering. This orthogonal method identifies deletions with
497 a PPV >90% for both WES and WGS, and identifies additional *de novo* deletions
498 compared to other SV callers.

499
500 When used with WES, we demonstrate that MEM has several advantages compared to
501 XHMM. First, MEM can be used on a single trio, while XHMM requires a minimum of 50
502 samples to accurately normalize read depth and calculate z-scores. Second, MEM
503 requires substantially less memory and runtime compared to XHMM. Third, MEM can
504 be used as a method for quality control, as it can identify UPD, sample mix-ups and
505 DNA contamination. MEM is also a worthwhile complementary tool to XHMM as MEM
506 identified additional *de novo* deletions that XHMM missed due to spurious evidence of
507 inheritance or seemingly inconsistent loss of exons. In addition, MEM identified
508 deletions with less than 3 exons with high precision, albeit with low sensitivity. The
509 combination of evidence from both XHMM and MEM can increase our ability to identify
510 smaller deletions with high precision and increased sensitivity, as well as reducing the
511 need for PCR-based validation, which is expensive and time-consuming.

512

513 CNV identification from WGS data is still under development. We propose MEM as a
514 worthwhile addition to the WGS CNV identification toolbox as it can be efficiently
515 implemented in less than a day and identifies deletions with a >90% PPV. It can be
516 implemented on a large cohort without significantly increasing the computational
517 requirements, and identifies additional *de novo* deletions compared to CNVnator,
518 Lumpy and SvABA. While there are other SV tools for WGS data (e.g., Delly, Pindel),
519 the methods utilized by CNVnator, Lumpy and SvABA, represent three primary ways to
520 identify CNVs: changes in read depth, discordant/split reads and local assembly, yet
521 MEM identified additional *de novo* deletions. Equally helpful is the orthogonal nature of
522 MEM, which may reduce the need for PCR validation for deletions identified by MEM
523 and a second tool.

524

525 MEM's primary limitation is the need for a complete trio, as many cohorts only recruit
526 singletons. The trio design is necessary in order to identify MEs and, therefore, cannot
527 be avoided. MEM is also limited regarding the size of the deletions it can detect with
528 high recall, which is a function of the SNV density in NGS data. WES deletions <200 kb
529 are identified with 24% recall, while deletions >200 kb are identified with 100% recall. Of
530 note, although the smaller deletions are not identified with high sensitivity, the PPV
531 remains high when they are called (78%). Based on deletions identified in GIAB AJ trio,
532 MEM identifies deletions from WGS with a range of sizes (100 – 660,000 bp); however,
533 we estimate that MEM has ~1% recall for deletions smaller than 3 kb and only 18%
534 recall for deletions 3-10 kb. Deletions >10 kb are identified with 45% recall. For this

535 reason MEM applied to WGS is particularly valuable as a secondary and orthogonal
536 method to confirm deletions identified by other tools, as the PPV is 92 - 97% with WGS
537 data.

538

539 MEM's sensitivity was also reduced by ME filtering, which accounted for ~5% of the
540 false negatives. Filtering is necessary in order to remove MEs caused by poor
541 genotyping or other errors and to achieve a high PPV. We suggest noting the number of
542 filtered MEs when verifying deletions identified with other tools, as even the presence of
543 1 or 2 MEs after filtering is evidence for a deletion in 88% of calls (data not shown).

544

545 Interestingly, 3.5% of regions with ME clusters identified with MEM were scored as
546 inherited duplications by ddPCR. Although ME genotypes are not indicative of a
547 duplication, it has been noted that some CNVs are complex events with multiple
548 breakpoints comprising both deletions and duplications in close proximity (Quinlan et
549 al., 2010). We hypothesize that this phenomenon likely underlies our observations, and
550 that in these few cases the primer placement for ddPCR targeted a region of duplication
551 rather than the deletion found by MEM.

552

553 The pursuit of disease-causing CNVs in family trios often focuses on the identification of
554 *de novo* or rare CNVs. MEM identifies both inherited and *de novo* deletions, however
555 one is unable to distinguish between inherited and *de novo* deletions without the use of
556 a secondary tool that identifies deletions in parents. In order to identify rare CNVs from
557 a large cohort, one must eliminate regions with deletions in the general population. This

558 is included in the MEM pipeline in Steps 4 and 5. If population data are not available,
559 one could determine the number of samples with deletions in each region identified by
560 MEM as an alternative. Deletion regions found in multiple samples are less likely to be
561 disease-causing.

562

563 We applied MEM to trios from the PCGC to identify deletions that are causal for CHD
564 that had not been seen with previous studies (Glessner et al., 2014). With MEM, we
565 identified and quantified two genetic mechanisms associated with CHD; BP1-BP2
566 deletions in 15q11.2 and UPD. Deletions in the region 15q11.2 BP1-BP2 account for
567 ~0.3% of CHD cases in the PCGC cohort. Although 15q11.2 deletions are associated
568 with a wide range of phenotypic anomalies, CHD have been reported in ~9% of carriers
569 (Cox and Butler, 2015), which explains the presence of an inherited mutation present in
570 both a proband with CHD and their apparently unaffected parent.

571

572 Using MEM, we also identified whole-chromosome maternal heterodisomy in ~0.3% of
573 CHD cases in the PCGC cohort. The likely genetic mechanism for maternal
574 heterodisomic UPDs is non-disjunction and subsequent trisomy rescue. Thus, there is a
575 possibility that probands with UPD may be mosaic for trisomy of the UPD chromosome,
576 and this mosaic trisomy could be the underlying cause of the probands' CHD. UPD
577 could also lead to CHD due to changes in methylation of imprinted genes. One example
578 from the chromosomes affected in PCGC probands is chromosome 8, which harbors
579 the known CHD gene *CHD7* (MIM:608892) that is maternally methylated (Joshi et al.,

580 2016). Maternal heterodisomy would lead to hypermethylation and altered expression of
581 *CHD7*.

582

583 In conclusion, MEM is an orthogonal tool that identifies deletion CNVs with over 90%
584 PPV and is a valuable addition to CNV detection pipelines for both WES and WGS. As
585 NGS data becomes more accessible, the need to identify CNVs from WES and WGS
586 data will only increase. This is particularly true with relation to disease causing CNVs as
587 CNVs have been implicated in a number of different human diseases including
588 congenital heart disease, schizophrenia, developmental delay and autism spectrum
589 disorders. MEM helps overcome some of the challenges associated with identifying
590 pathogenic CNVs due to limited specificity of current SV tools.

591

592 **Acknowledgments**

593 The authors are grateful to the patients and families who participated in this research
594 and team members who supported subject recruitment and sequencing D. Awad, C.
595 Breton, K. Celia, C. Duarte, D. Etwaru, N. Rishman, M. Daspakova, J. Kline, R. Korsin,
596 A. Lanz, E. Marquez, D. Queen, A. Rodriguez, J. Rose, J.K. Sond, D. Warburton, A.
597 Wilpers and R. Yee (Columbia Medical School); B. McDonough, A. Monafo, J. Stryker
598 (Harvard Medical School); N. Cross (Yale School of Medicince); S. M. Edman, J.L.
599 Garbarini, J.E. Tusi, S.H. Woyciechowski (Children's Hospital of Philadelphia); J.
600 Ellashek and N. Tran (Children's Hospital of Los Angeles); K. Flack, L. Panesar, N.
601 Taylor (Univeristy College London); D. Gruber and N. Stellato (Steve and Alexandra
602 Cohen Children's Medical Center of New York); D. Guevara, A. Julian, M. MacNeal, C.

603 Mintz (Icahn School of Medicine at Mount Sinai); and E. Taillie (University of Rochester
604 School of Medicine and Dentistry). We also thank the Simons Foundation for Autism
605 Research for the contribution of SSC exome trios. This work was supported by grants
606 from the National Heart, Lung, and Blood Institute (NHLBI) for the Pediatric Cardiac
607 Genomics Consortium (U01-HL098188, U01-HL131003, UM1-HL098147, UM1-
608 HL098153, UM1-HL098163, UM1-HL098123, UM1-HL098162, UM1-HL128761, UM1-
609 HL128711). The views expressed are those of the authors and do not necessarily
610 reflect those of the NHLBI. Research reported in this paper was supported by the Office
611 of Research Infrastructure of the National Institutes of Health under award number
612 S10OD018522. This work was supported in part through the computational resources
613 and staff expertise provided by Scientific Computing at the Icahn School of Medicine at
614 Mount Sinai.

615
616 **Conflict of Interest:** The authors have no conflicts of interest to declare.
617
618 **Ethical compliance:** All procedures performed in studies involving human participants
619 were in accordance with the ethical standards of the following Institutional Review
620 Boards: Boston Children's Hospital, Brigham and Women's Hospital, Great Ormond
621 Street Hospital, Children's Hospital of Los Angeles, Children's Hospital of Philadelphia,
622 Columbia University Medical Center, Icahn School of Medicine at Mount Sinai,
623 Rochester School of Medicine and Dentistry, Steven and Alexandra Cohen Children's
624 Medical Center of New York, and Yale School of Medicine. Informed consent was
625 obtained from all individual participants or their parent/guardian included in this study.

626

627 **References**

628 Abyzov A, Urban AE, Snyder M, Gerstein M. 2011. CNVnator: An approach to discover,
629 genotype, and characterize typical and atypical CNVs from family and population
630 genome sequencing. *Genome Res* 21:974–984.

631 Bandler WM, Antaki D, Gujral M, Noor A, Rosario G, Chapman TR, Barrera DJ, Lin
632 GN, Malhotra D, Watts AC, Wong LC, Estabillo JA, et al. 2015. Frequency and
633 complexity of de novo structural mutation in autism. *bioRxiv* 1–19.

634 Cafferkey M, Ahn JW, Flinter F, Ogilvie C. 2014. Phenotypic Features in Patients With
635 15q11.2(BP1-BP2) Deletion: Further Delineation of an Emerging Syndrome. *Am J Med
636 Genet Part A* 2:1916–1922.

637 Conrad DF, Pinto D, Redon R, Feuk L, Gokcumen O, Zhang Y, Aerts J, Andrews TD,
638 Barnes C, Campbell P, Hu M, Ihm CH, et al. 2012. Origins and functional impact of copy
639 number variation in the human genome. *464*:704–712.

640 Cox DM, Butler MG. 2015. The 15q11.2 BP1-BP2 microdeletion syndrome: A review. *Int
641 J Mol Sci* 16:4068–4082.

642 Fromer M, Purcell SM. 2014. Using XHMM Software to Detect Copy Number Variation
643 in Whole-Exome Sequencing Data. *Curr Protoc Hum Genet* 81:7.23.1-7.23.21.

644 Gilissen C, Hehir-Kwa JY, Thung DT, Vorst M van de, Bon BWM van, Willemsen MH,
645 Kwint M, Janssen IM, Hoischen A, Schenck A, Leach R, Klein R, et al. 2014. Genome
646 sequencing identifies major causes of severe intellectual disability. *Nature* 511:344–
647 347.

648 Glessner J, Bick AG, Ito K, Homsy J, Rodriguez-Murillo L, Fromer M, Mazaika EJ,

649 Vardarajan B, Italia MJ, Leipzig J, DePalma S, Golhar R, et al. 2014. Increased
650 frequency of de novo copy number variations in congenital heart disease by integrative
651 analysis of SNP array and exome sequence data. *Circ Res.*
652 Homsy J, Zaidi S, Shen Y, Ware JS, Samocha KE, Karczewski KJ, Depalma SR,
653 McKean D, Wakimoto H, Gorham J, Jin SC, Deanfield J, et al. 2015. De novo mutations
654 in congenital heart disease with neurodevelopmental and other congenital anomalies.
655 *Science* (80-) 350:1262–1266.
656 Iossifov I, O'Roak BJ, Sanders SJ, Ronemus M, Krumm N, Levy D, Stessman HA,
657 Witherspoon K, Vives L, Patterson KE, Smith JD, Paeper B, et al. 2014. The
658 contribution of de novo coding mutations to autism spectrum disorder. *Nature* 13:216–
659 221.
660 Jeffares DC, Jolly C, Hoti M, Speed D, Shaw L, Rallis C, Sedlazeck FJ. 2017. Transient
661 structural variations have strong effects on quantitative traits and reproduction isolation
662 in fission yeast. *Nat Commun* 1–11.
663 Joshi RS, Garg P, Zaitlen N, Lappalainen T, Watson CT, Azam N, Ho D, Li X,
664 Antonarakis SE, Brunner HG, Buiting K, Cheung SW, et al. 2016. DNA Methylation
665 Profiling of Uniparental Disomy Subjects Provides a Map of Parental Epigenetic Bias in
666 the Human Genome. *Am J Hum Genet* 99:555–566.
667 Jun G, Flickinger M, Hetrick KN, Romm JM, Doheny KF, Abecasis GR, Boehnke M,
668 Kang HM. 2012. Detecting and estimating contamination of human DNA samples in
669 sequencing and array-based genotype data. *Am J Hum Genet* 91:839–48.
670 Kloosterman WP, Francioli LC, Hormozdiari F, Marschall T, Hehir-kwa JY, Abdellaoui A,
671 Lameijer E, Moed MH, Koval V, Renkens I, Roosmalen MJ Van, Arp P, et al. 2015.

672 Characteristics of de novo structural changes in the human genome. *Genome Res* 792–
673 801.

674 Layer RM, Chiang C, Quinlan AR, Hall IM. 2014. LUMPY: a probabilistic framework for
675 structural variant discovery. *Genome Biol* 15:R84.

676 Mazaika E, Homsy J. 2014. Digital Droplet PCR: CNV Analysis and Other Applications.
677 *Curr Protoc Hum Genet* 82:7.24.1-7.24.13.

678 McCarroll S a, Hadnott TN, Perry GH, Sabeti PC, Zody MC, Barrett JC, Dallaire S,
679 Gabriel SB, Lee C, Daly MJ, Altshuler DM, The International HapMap Consortium.
680 2006. Common deletion polymorphisms in the human genome. *Nat Genet* 38:86–92.

681 Mccarroll SA, Hadnott TN, Perry GH, Sabeti PC, Zody MC, Barrett JC, Dallaire S,
682 Gabriel SB, Lee C, Daly MJ, Altshuler DM, Hapmap I. 2006. Common deletion
683 polymorphisms in the human genome. 38:86–92.

684 O'Roak BJ, Deriziotis P, Lee C, Vives L, Schwartz JJ, Girirajan S, Karakoc E,
685 Mackenzie AP, Ng SB, Baker C, Rieder MJ, Nickerson D a, et al. 2011. Exome
686 sequencing in sporadic autism spectrum disorders identifies severe de novo mutations.
687 *Nat Genet* 43:585–9.

688 Quinlan AR, Clark RA, Sokolova S, Leibowitz ML, Zhang Y, Hurles ME, Mell JC, Hall
689 IM. 2010. Genome-wide mapping and assembly of structural variant breakpoints in the
690 mouse genome. *Genome Res* 623–635.

691 Sanders SJ, Murtha MT, Gupta AR, Murdoch JD, Raubeson MJ, Willsey AJ, Ercan-
692 Sencicek AG, DiLullo NM, Parikshak NN, Stein JL, Walker MF, Ober GT, et al. 2012. De
693 novo mutations revealed by whole-exome sequencing are strongly associated with
694 autism. *Nature* 485:237–241.

695 Szatkiewicz JP, O'Dushlaine C, Chen G, Chambert K, Moran JL, Neale BM, Fromer M,
696 Ruderfer D, Akterin S, Bergen SE, Kähler a, Magnusson PKE, et al. 2014. Copy
697 number variation in schizophrenia in Sweden. Mol Psychiatry 19:762–73.
698 Tattini L, D'Aurizio R, Magi A. 2015. Detection of genomic structural variants from next-
699 generation sequencing data. Front Bioeng Biotechnol 3:.
700 Wala J, Bandopadhyay P, Greenwald N, Rourke RO, Stewart C, Schumacher S, Li Y,
701 Weischenfeldt J, Nusbaum C, Campbell P, Meyerson M, Zhang Z. 2017. SvABA:
702 Genome-wide detection of structural variants and indels by local assembly. bioRxiv 1–
703 40.
704 Weischenfeldt J, Symmons O, Spitz F, Korbel JO. 2013. Phenotypic impact of genomic
705 structural variation□: insights from and for human disease. Nat Rev Genet 14:125–138.
706 Weisenfeld NI, Yin S, Sharpe T, Lau B, Hegarty R, Holmes L, Sogoloff B, Tabbaa D,
707 Williams L, Russ C, Nusbaum C, Lander ES, et al. 2014. Comprehensive variation
708 discovery in single human genomes. Nat Publ Gr 46:1350–1355.
709 Werling DM, Brand H, An J-Y, Stone MR, Glessner JT, Zhu L, Collings RL, Dong S,
710 Layer RM, Markenscoff-Papadimitriou E, Farrell A, Schwartz GB, et al. 2017. Limited
711 contribution of rare, noncoding variation to autism spectrum disorder from sequencing of
712 2,076 genomes in quartet families. bioRxiv 1–45.
713 Zook JM, Catoe D, McDaniel J, Vang L, Spies N, Sidow A, Weng Z, Liu Y, Mason CE,
714 Alexander N, Henaff E, McIntyre ABR, et al. 2016. Data Descriptor□: Extensive
715 sequencing of seven human genomes to characterize benchmark reference materials.
716 Nature 1–26.
717

718 **Figure Legends**

719 **Figure 1: Schematic of MEM principle.** Diagram of trio where proband inherited a
720 deletion from parent 1. Tools report homozygous genotypes (red) that violate Mendelian
721 laws of segregation in the case of hemizygosity due to a heterozygous deletion.

722 Adapted from McCarroll *et al.* 2006 (McCarroll *et al.*, 2006).

723

724 **Figure 2: MEM pipeline for WES and WGS data.**

725

726 **Figure 3:** A) Comparison of *de novo* deletions called by XHMM and MEM. B) Size
727 distribution of *de novo* deletions called by XHMM. Colors in stacked histogram indicate
728 which tools detected the deletion (red = MEM and XHMM detected, green = MEM
729 detected and not XHMM, blue = XHMM detected and not MEM).

730

731 **Figure 4: MEs plotted by chromosome** A) MEs in a trio after quality filtering. B)
732 Sample with UPD on chromosome 9. C) Trio with DNA contamination. D) Trio with a
733 sample mix.

734

735

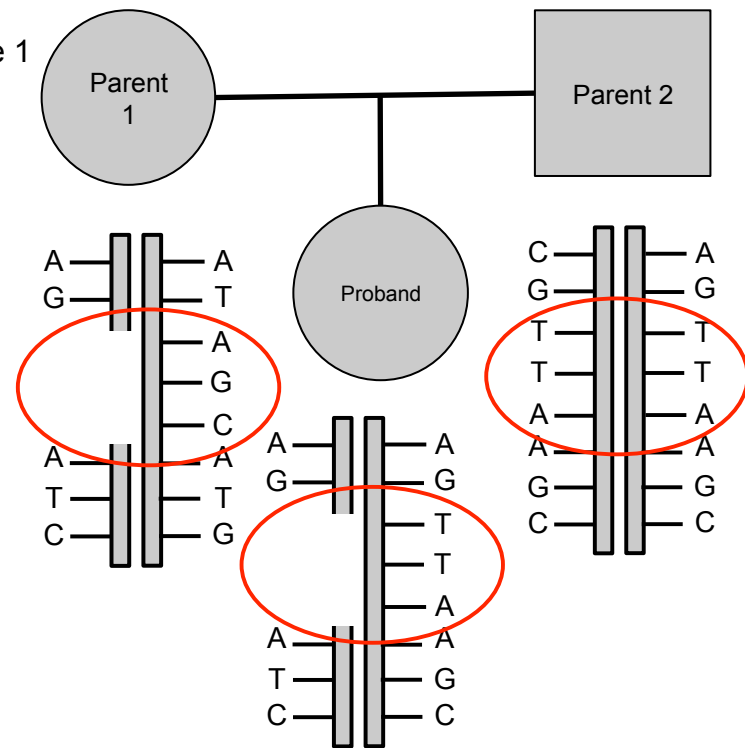
736

737

738

739

Figure 1



Parent 1	Parent 2	Expected in Child	Observed in Child
AA	TT	AT	TT
GG	TT	GT	TT
CC	AA	CA	AA

Figure 2

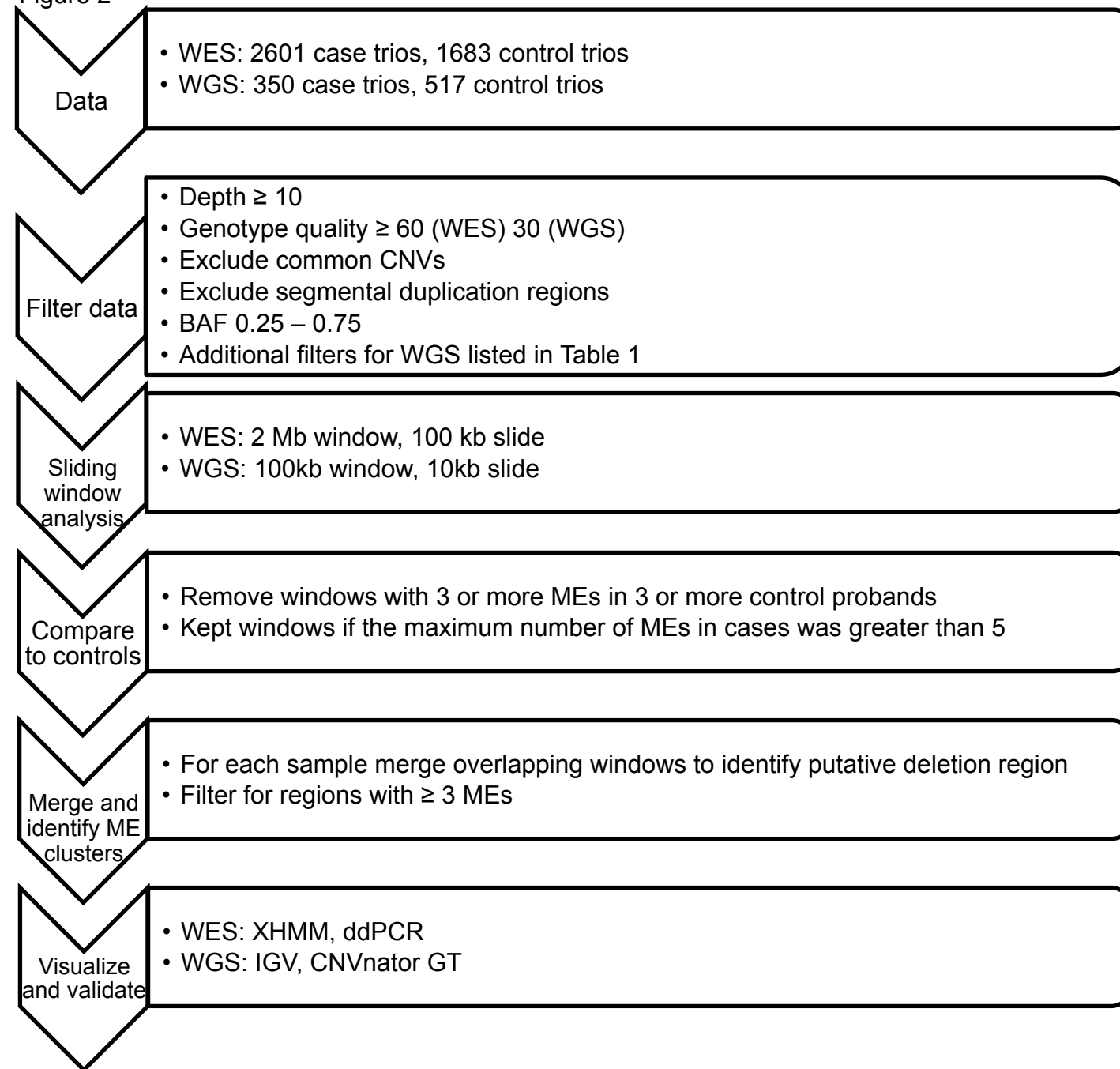
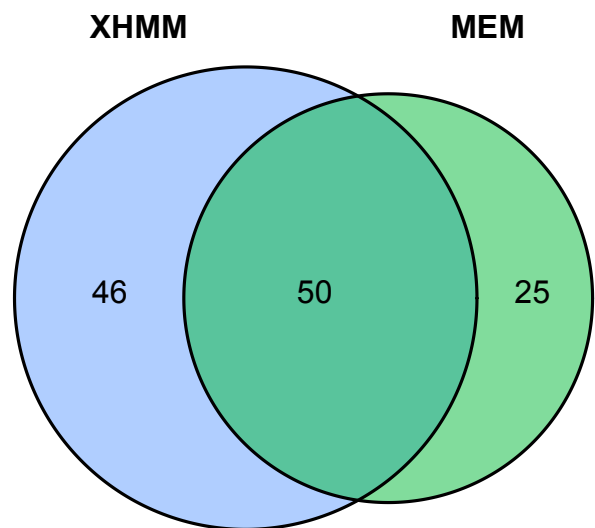


Figure 3

A



B

Size distribution of de novo deletions detected by MEM and XHMM

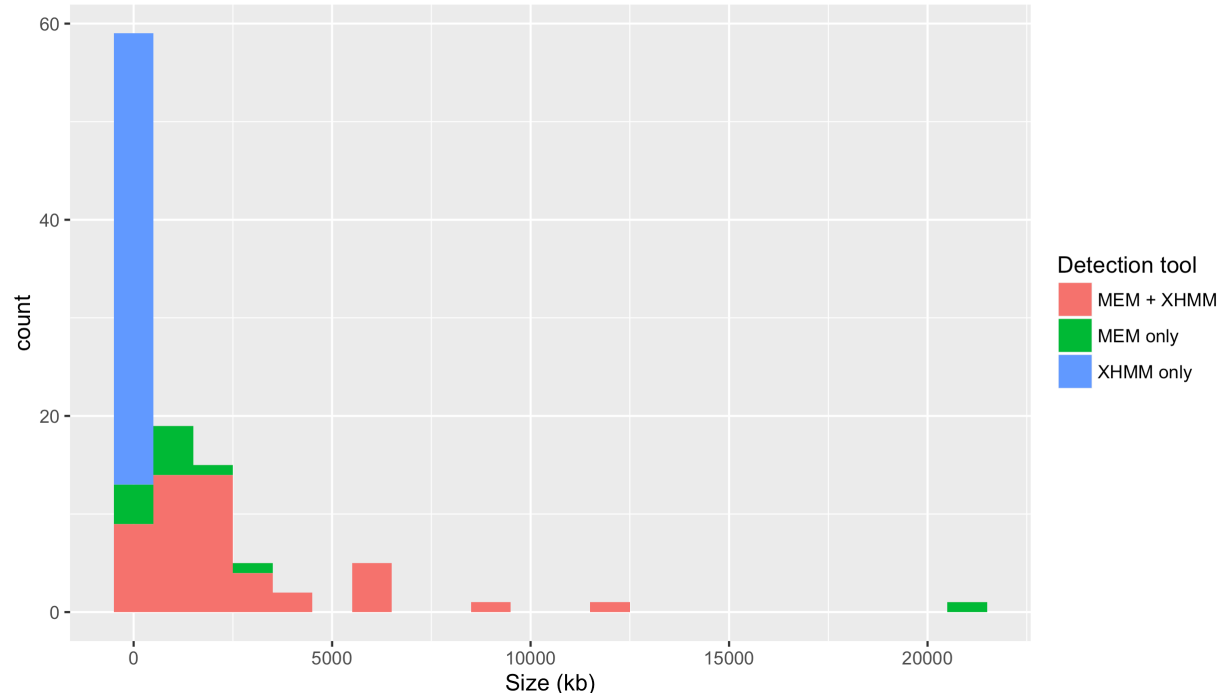
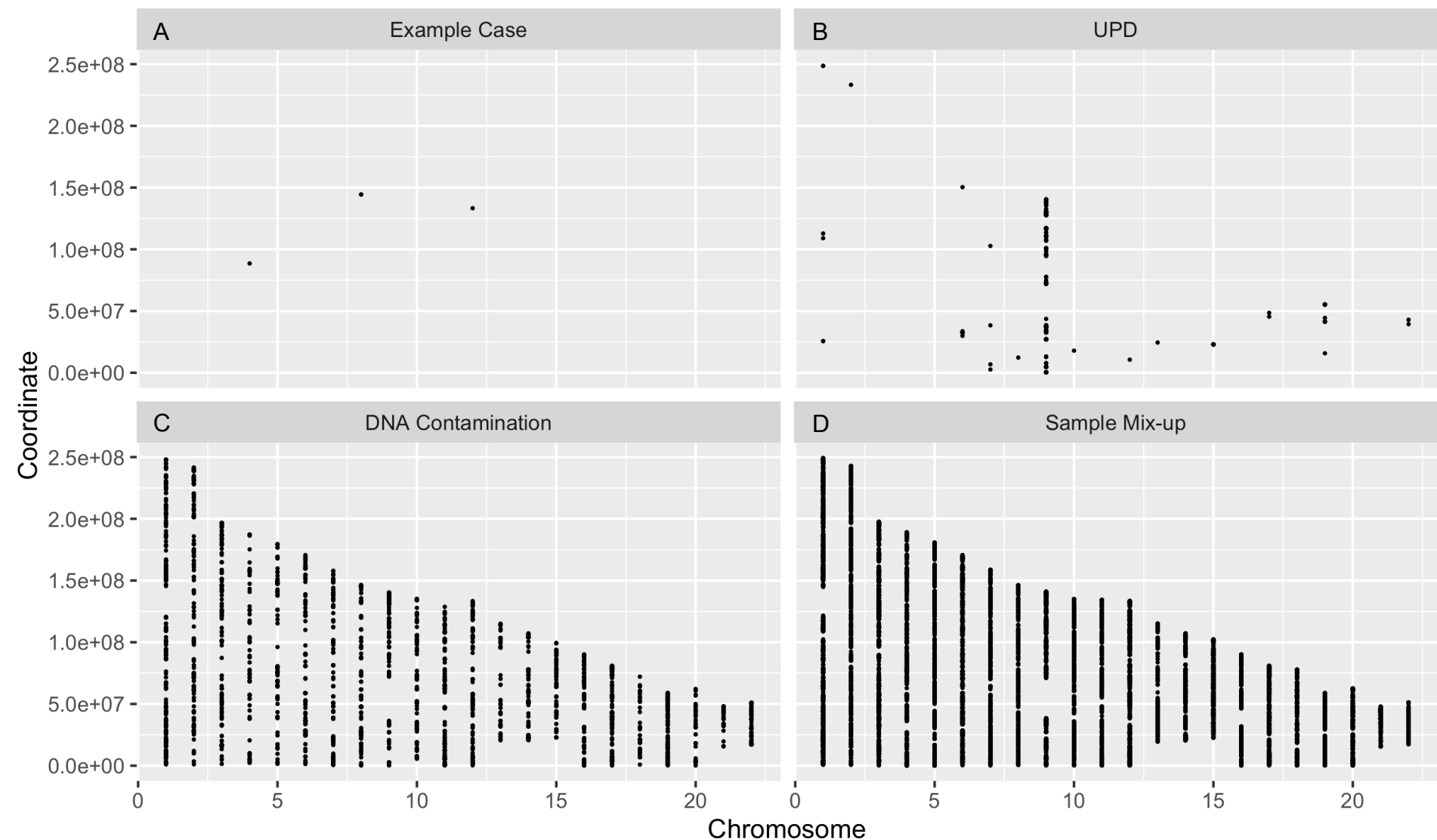


Figure 4



Tables

Table 1: Computational resources required for NGS CNV detection tools

Tool	Runtime (seconds)	Max Memory (MB)	Average Memory (MB)
MEM WES	5.5	21	12
XHMM	453	278	81
MEM WGS	407	21	7
CNVnator	77,629	7,674	709
Lumpy/SVTyper	4,238	12,876	4,898